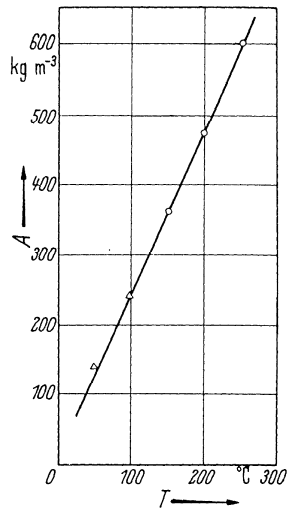

Fig. 32A-1-001. KIO_3. *A* vs. *T* [61Her]. *A*: solubility in water (solute/solvent).

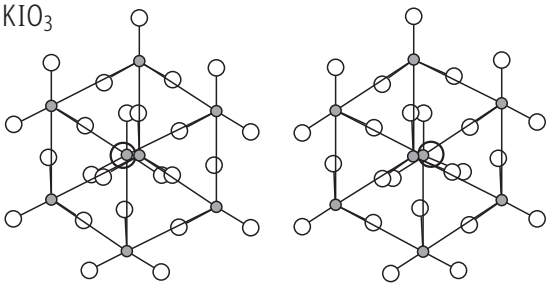

Fig. 32A-1-002. KIO_3. Crystal structure of phase I at T = 523 K [87Byr]. A stereo view approximately along [111] direction with *c* axis vertical. Space group: R3– C_3^4. IO_3 groups are distinguished. The atoms are represented by circles of reducing size: K, O, I, respectively.

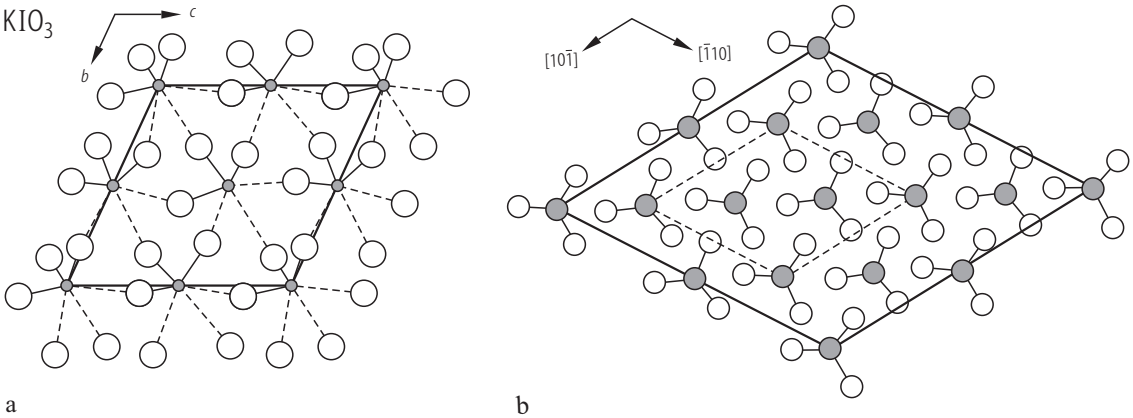

Fig. 32A-1-003. KIO_3. Crystal structure of phase III at RT [78Kal]. (**a**) Projection along *a* axis with IO_3 groups distinguished. Dashed lines indicate longer I–O bonds of 2.63...2.83 Å in length. The potassium atoms locate above or below the iodine atoms. (**b**) Projection along [111]. Rhombohedral pseudocell is drawn by dashed lines.

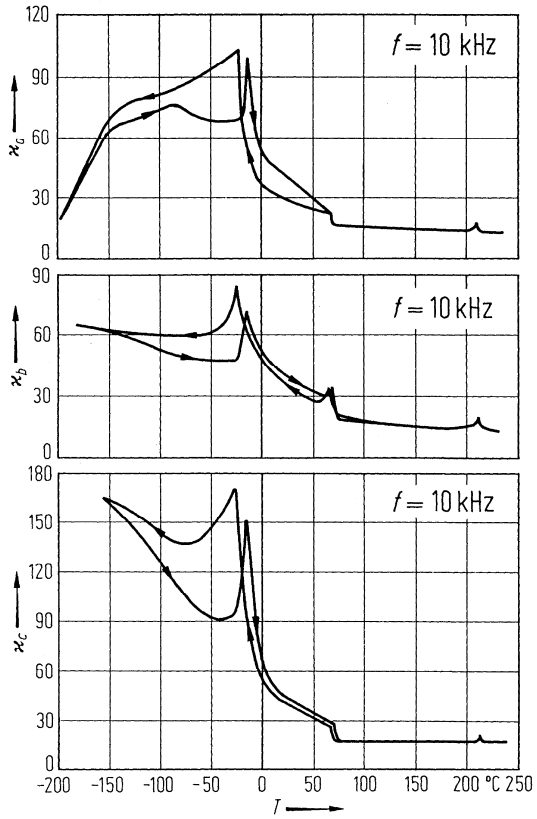

Fig. 32A-1-004. KIO_3. κ_a, κ_b, κ_c vs. T [70Hel]. f = 10 kHz. The axes a, b, c refer to the pseudocubic cell.

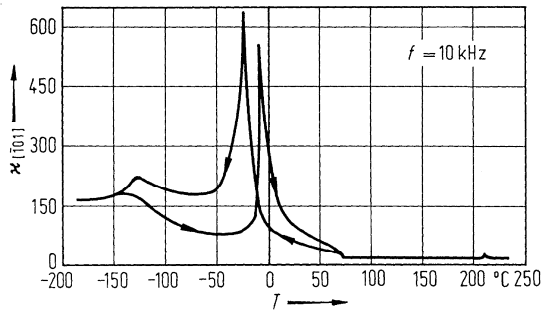

Fig. 32A-1-005. KIO_3. $\kappa_{[\bar{1}01]}$ vs. T [70Hel]. f = 10 kHz. $[\bar{1}01]$ refers to the pseudocubic cell.

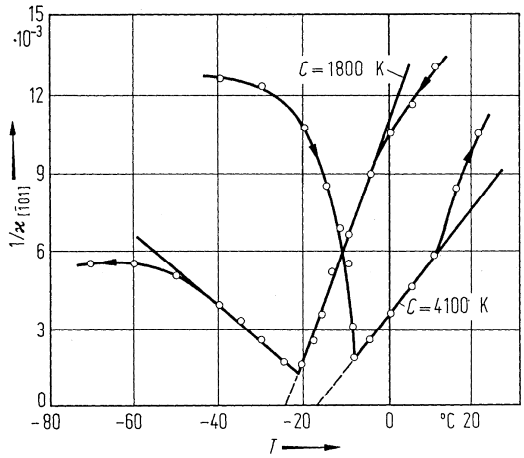

Fig. 32A-1-006. KIO_3. $\kappa^{-1}_{[\bar{1}01]}$ vs. T [70Hel]. f = 10 kHz. $[\bar{1}01]$ refers to the pseudocubic cell. The two curves correspond to different treatment of specimens. C: Curie-Weiss constant.

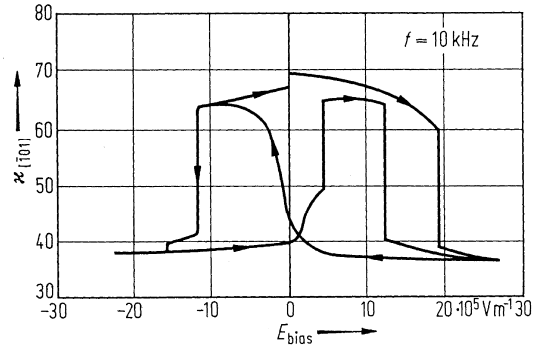

Fig. 32A-1-007. KIO_3. $\kappa_{[\bar{1}01]}$ vs. E_{bias} [70Hel]. f = 10 kHz. T = 22 °C. $[\bar{1}01]$ refers to the pseudocubic cell.

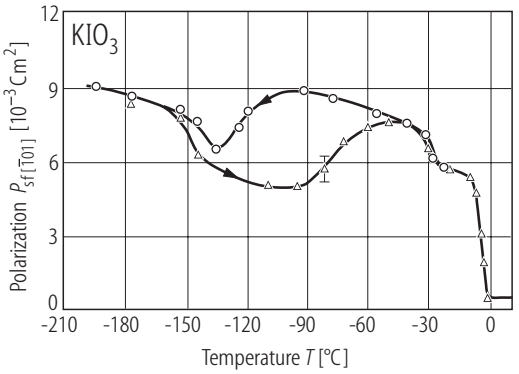

Fig. 32A-1-008. KIO_3. $P_{sf[\bar{1}01]}$ vs. T [70Hel]. $\boldsymbol{E} \parallel [\bar{1}01]$. $[\bar{1}01]$ refers to the pseudocubic cell. $P_{sf[\bar{1}01]} = \sqrt{3}\, P_{sf}/2$.

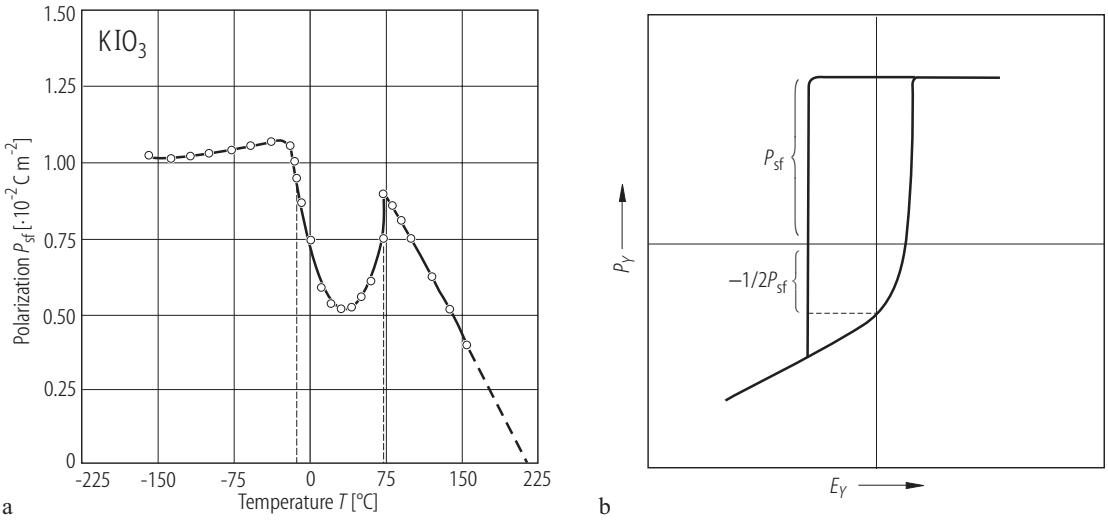

Fig. 32A-1-009. KIO_3. (**a**) P_{sf} vs. T, (**b**) the hysteresis loop [73Shu]. Y-cut specimen. Dashed lines in (**a**) indicate Θ_{IV-III} and Θ_{III-II}. See subsection 2b for orthogonal coordinate system.

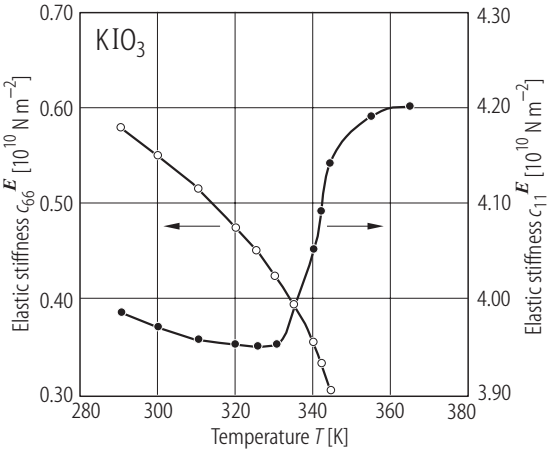

Fig. 32A-1-010. KIO_3. c_{66}^E, c_{11}^E vs. T [95Hau]. See subsection 2b for orthogonal coordinate system.

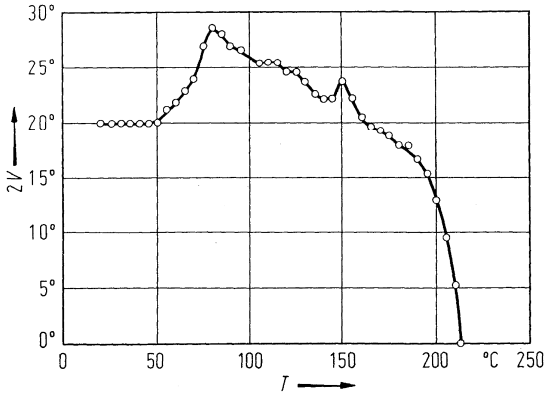

Fig. 32A-1-011. KIO_3. $2V$ vs. T [72Cra]. $2V$: optical axial angle.

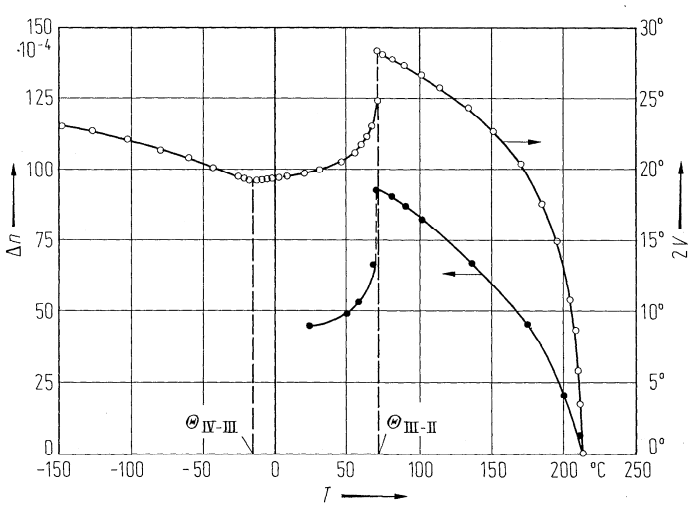

Fig. 32A-1-012. KIO_3. Δn, $2V$ vs. T [73Shu]. $\Delta n = n_Y - n_X$. $2V$: optical axial angle. See subsection 2b for orthogonal coordinate system.

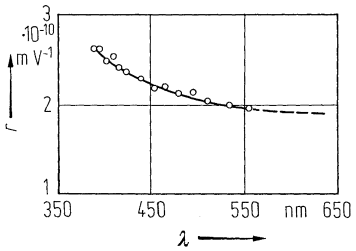

Fig. 32A-1-013. KIO_3. r vs. λ [73Shu]. $r = r_{12} - (n_Y/n_X)^3 r_{22}$. T = 20 °C. See subsection 2b for orthogonal coordinate system.

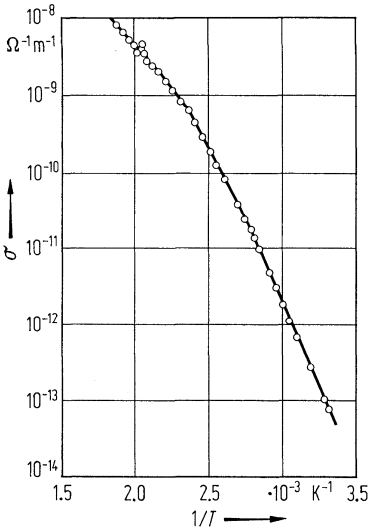

Fig. 32A-1-014. KIO_3. σ vs. $1/T$ [69Gur]. Conductivity σ was measured in dry air by the two-terminal method with vacuum evaporated Ag electrodes. Applied field E = 120 kV m^{-1}.

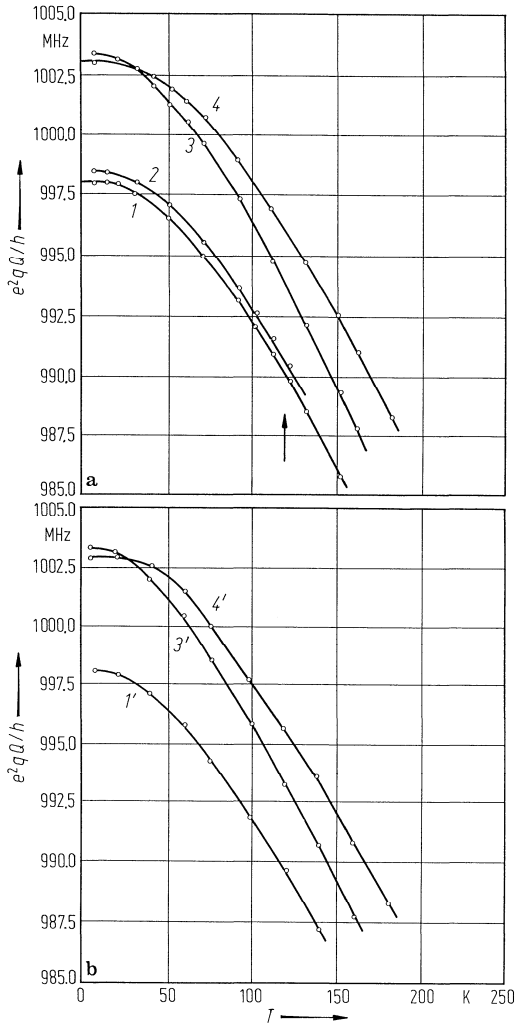

Fig. 32A-1-015. KIO_3. e^2Qq/h vs. T [82Bai]. e^2Qq/h: ^{127}I quadrupole coupling constants determined by multiple lines. (**a**) HIO_3 doped single crystal, (**b**) chemically pure polycrystalline specimen.

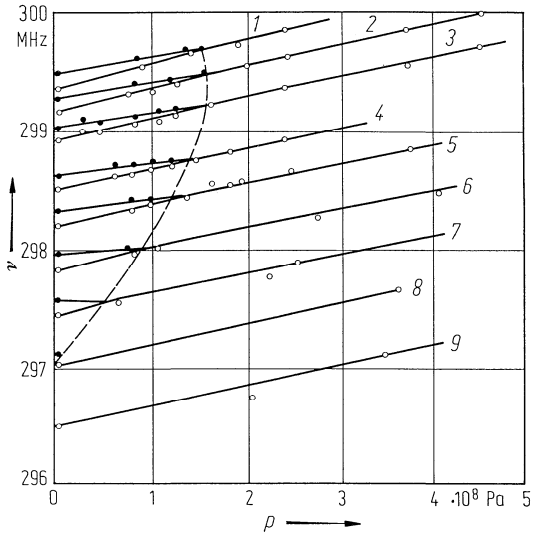

Fig. 32A-1-016. KIO_3. ν vs. p [82Bai]. HIO_3 doped specimen. ν: NQR frequency of $^{127}I(\pm 3/2 \leftrightarrow \pm 5/2)$ transition. Parameter: T; curve *1*: 4.2...20 K, *2*: 40 K, *3*: 60 K, *4*: 77 K, *5*: 90 K, *6*: 100 K, *7*: 110 K, *8*: 120 K, *9*: 130 K. Open and closed circles represent the transitions corresponding to the lines *1* and *2* of Fig. 32A-1-015(**a**), respectively.

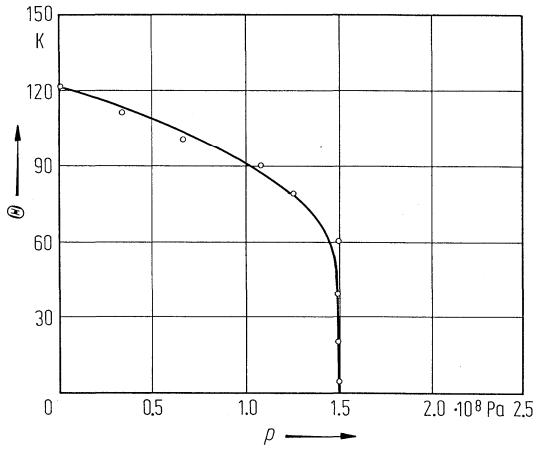

Fig. 32A-1-017. KIO_3. Θ vs. p [82Bai]. HIO_3 doped specimen. Θ, p: temperature and pressure at which the multiplicity in the ^{127}I NQR spectrum changes; see Fig. 32A-1-016.

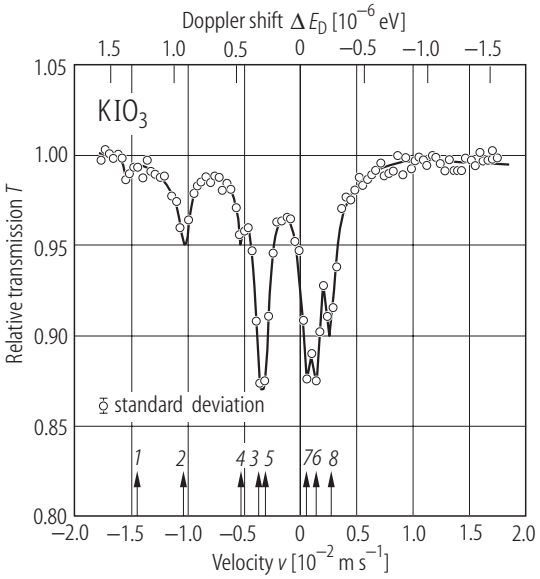

Fig. 32A-1-018. KIO_3. Relative transmission vs. v, ΔE_D at T = 80 K [63DeW]. v: source velocity. ΔE_D: Doppler shift. The absorber is $K^{129}IO_3$, the source is $^{66}Zn^{129}Te$. The arrows indicate the calculated positions of the hyperfine components.

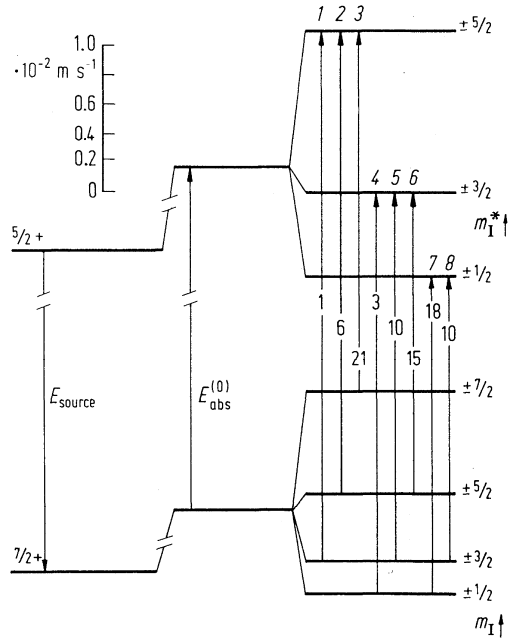

Fig. 32A-1-019. KIO_3. Nuclear energy levels for ground and first excited states of ^{129}I and KIO_3 [63DeW]. T = 80 K. m, m^*: magnetic quantum number of ground and excited states.